Probing proteasome activity and function : cancer diagnostics and mechanism of antigen processing

Berkers, C.R.

Chapter 2.1

Comparison of the specificity and activity profiles of the proteasome inhibitors bortezomib and CEP-18770

Submitted

Comparison of the specificity and activity profiles of the proteasome inhibitors bortezomib and CEP-18770

Celia R. Berkers,[a] Karianne G. Schuurman,[a] Yves Leestemaker,[a] Bruce Ruggeri,[b] Susan Jones-Bolin,[b] Michael Williams[b] & Huib Ovaa[a,*]

[a]Division of Cell Biology II, The Netherlands Cancer Institute, Plesmanlaan 121, 1066 CX Amsterdam, The Netherlands. [b]Cephalon Inc, Discovery Research, West Chester, PA, USA.

The ubiquitin proteasome system is an attractive pharmacological target for the treatment of cancer. The proteasome inhibitor bortezomib has been approved for the treatment of multiple myeloma (MM) and mantle cell lymphoma, but is associated with substantial adverse effects and the occurrence of resistance, underscoring the continued need for novel proteasome inhibitors. In this study, bortezomib and the novel proteasome inhibitor CEP-18770 were compared for their ability to inhibit proteasome activity using both fluorogenic substrates and a recently developed chemical proteasome activity probe. Bortezomib and CEP-18770 were equipotent in inhibiting distinct subunits of the proteasome in a panel of cell lines *in vitro*. In a preclinical MM model, both inhibitors inhibited the proteasome in normal tissues to a similar extent. Tumor proteasome activity was inhibited to a significantly higher extent by CEP-18770 (60%) compared to bortezomib (32%). In addition, CEP-18770 was able to overcome bortezomib resistance *in vitro*. The present findings demonstrate that proteasome activity probes can accurately monitor the effects of proteasome inhibitors on both normal and tumor tissues in preclinical models. Furthermore, the data presented here indicate that CEP-18770 has a favorable pharmacodynamic profile compared to bortezomib, and provide rationale for further clinical development of CEP-18770.

INTRODUCTION

The ubiquitin-proteasome system is responsible for the degradation of proteins involved in a wide variety of cellular processes, including cell proliferation and survival, cell-cycle control, transcriptional regulation and cellular stress responses, as well as for the destruction of abundant and misfolded proteins.[1,2] The catalytic activity of the 26S proteasome resides within its 20S core and is mediated by three catalytically active constitutive β-subunits termed β1, β2, and β5. These have three different catalytic activities, caspase-like, tryptic and chymotryptic activity, respectively. In lymphoid tissues or after induction with interferon γ, these subunits can be replaced by their immunoproteasomal counterparts, termed β1i, β2i, and β5i, to form the immunoproteasome, while mixed-type hybrid proteasomes have also been reported.[3-6] The increased sensitivity of malignant cells to proteasome inhibitors has resulted in proteasome inhibition emerging as a novel strategy

*Correspondence should be addressed to H.O. (h.ovaa@nki.nl).

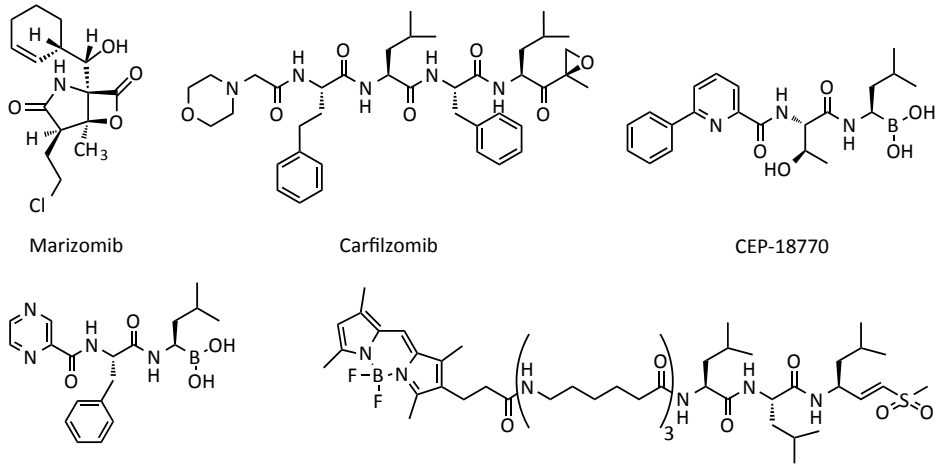

Figure 1 | Structures of bortezomib, CEP-18770, NPI-0052, carfilzomib and proteasome activity probe 1 (Me_4BodipyFL-Ahx_3Leu_3VS).

for cancer treatment.[2] In addition to eliciting direct apoptotic effects, proteasome inhibition may also enhance sensitivity and overcome drug resistance to standard chemo- and radiation therapy.[7] Bortezomib[8] (Figure 1), the active ingredient of velcade®, was the first proteasome inhibitor to be approved as a single agent for the treatment of relapsed or refractory multiple myeloma (MM)[9-11] and mantle cell lymphoma[12] and, in combination with PEGylated doxorubicin, for the treatment of relapsed MM.[13,14] Bortezomib induces apoptosis via stabilization of a number of proapoptotic and/or regulatory proteins. Both stabilization of p53 and inhibition of NF-κB (nuclear factor κB) mediated transcription via stabilization of its inhibitor IκBα, are thought to play important roles in bortezomib-induced apoptosis,[15,16] although additional mechanisms have been implicated to explain the anti-tumor efficacy of bortezomib.[17,18]

Bortezomib treatment is associated with manageable but substantial side effects e.g., thrombocytopenia and peripheral neuropathy[10] and the occurrence of both primary and acquired drug-resistance.[18] Consequently, there is an ongoing need for the development of novel proteasome inhibitors, and several second-generation proteasome inhibitors are now entering clinical trials. These include carfilzomib (PR-171),[19-21] an irreversible epoxyketone peptidyl inhibitor, and marizomib (NPI-0052),[22,23] an orally available proteasome inhibitor isolated from the marine actinomycete, *Salinispora spp* (Figure 1). Both these inhibitors demonstrate a favorable cytotoxicity profile as compared to bortezomib and can overcome bortezomib resistance *in vitro*.[19,20,22]

Another second-generation proteasome inhibitor in clinical development is CEP-18770[24] (Figure 1). Like bortezomib, CEP-18770 is a reversible boronic acid-based inhibitor that suppresses NF-κB-mediated transcription, and induces apoptosis in human MM cell lines and patient derived cells to a similar extent.[25] It has a favorable cytotoxicity profile towards a variety of normal human cell lines as compared to bortezomib.[25] In a preclinical model of human MM, CEP-18770 evidenced significant and sustained proteasome inhibi-

tion in tumors relative to normal tissues and anti-tumor efficacy, resulting in complete tumor regression of MM xenografts.[25] Importantly, CEP-18770 is orally bioavailable, and oral administration of CEP-18770 resulted in significant reduction in tumor weight and dose-related incidence of complete tumor regression with minimal changes in animal body weight.[25,26]

In the present study, the proteasome inhibitory capacities of bortezomib and CEP-18770 were profiled side by side *in vitro* and in a variety of *in vivo* preclinical models, using both fluorogenic substrates and a recently developed chemical proteasome activity probe, that allows profiling of all constitutive and immunoproteasomal activities in live cells and *ex vivo*.[27] These studies demonstrate that both bortezomib and CEP-18770 inhibit β1 and β5 subunits to a similar extent in a panel of multiple myeloma cell lysates and cells. Furthermore, in a preclinical model of human MM, CEP-18770 inhibited tumor proteasome activity to a significantly higher extent (60% inhibition of total activity) compared to bortezomib (32% inhibition of total activity), while CEP-18770 inhibited the proteasome in normal tissues with equal potency compared to bortezomib. Finally, our data show that CEP-18770 is able to overcome bortezomib resistance *in vitro*.

RESULTS

Bortezomib and CEP-18770 show comparable inhibition profiles in a panel of cell lysates

CEP-18770 and bortezomib are chemically related (Figure 1) and have a comparable ability to induce apoptosis in MM cell lines and in purified primary human MM explants cultures, but show substantial differences in their cytotoxicity profile towards normal cells and in their antitumor-efficacy.[25] To assess whether these differences can be related to differences in proteasome inhibition, the proteasome inhibitory potential of CEP-18770 and bortezomib were first compared in cell lysates using fluorogenic substrates for the different proteasomal activities. Lysates from RPMI8226, H929, JJN3 (all MM) and HeLa (cervical carcinoma) cells were pre-incubated for 1 hour with increasing concentrations of CEP-18770 and bortezomib after which residual proteasome activity was measured (Figure 2A). IC_{50} values for the chymotryptic and caspase-like activities of the proteasome were calculated (Figure 2B). Bortezomib (black lines) and CEP-18770 (grey lines) showed almost identical inhibition profiles in all cell lines tested (Figure 2A) and inhibited both the chymotryptic activity (thin solid lines) and the caspase-like activity (dotted lines), but not the tryptic activity (thick solid lines), as has been described for bortezomib.[25,28] IC_{50} values for inhibition of the chymotryptic activity were 10–25 nM depending on the cell line used and did not differ significantly between bortezomib and CEP-18770 (Figure 2B). When IC_{50} values were compared between different tumor cell lines, RPMI8226 and H929 MM cells were more sensitive than JJN3 and HeLa cells to inhibition of chymotryptic activity. Whereas in RPMI8226 and H929 cells IC_{50} values between 9 and 13 nM were measured, HeLa and JJN3 cells required 20–24 nM of CEP-18770 or bortezomib for 50% inhibition (Figure 2B). Consistent with the finding that low concentrations of CEP-18770 inhibit the proteasome to a higher extent in H929 or RPMI8226 cells compared to JJN3 cells, a low concentration of CEP-18770 induced apoptosis in RPMI8226 and H929 cells, but not in JJN3 cells.[25] IC_{50} values for inhibition of the caspase-like activity were 40–75 nM depending on the cell line used. CEP-18770 was more specific for the chymotryptic activity as compared to bortezomib in both JJN3 and HeLa cells, but a significant difference between IC_{50} values ($p<0.05$) was only

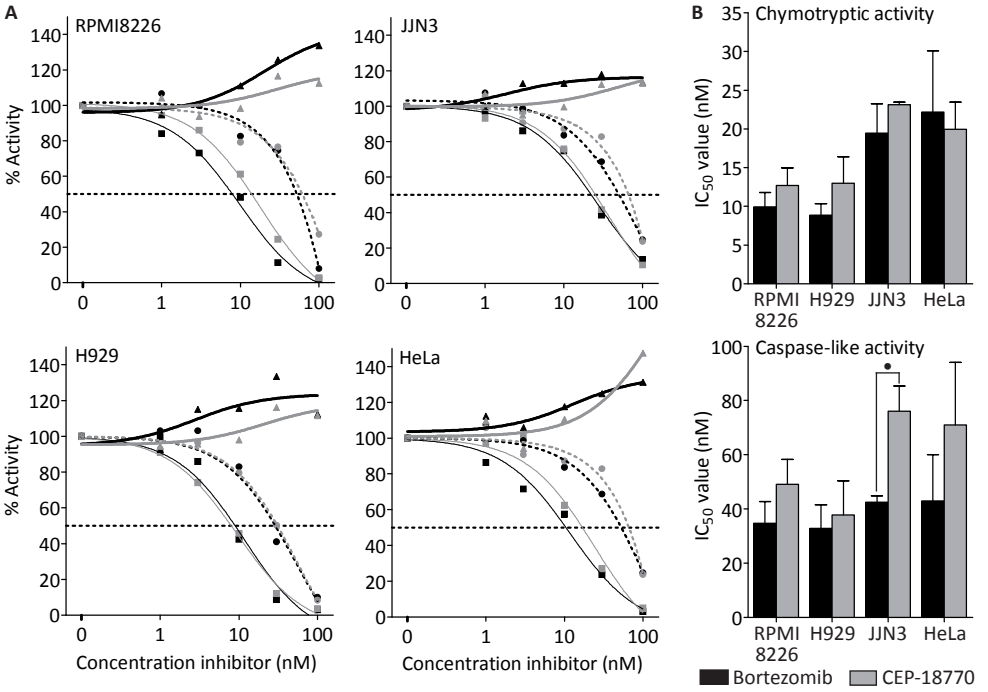

Figure 2 | Bortezomib and CEP-18770 have identical proteasome inhibition profiles in cell lysates. A) Representative proteasome inhibitory profiles in RPMI8226, H929, JJN3 and HeLa cell lysates after addition of increasing concentrations of bortezomib (black lines) or CEP-18770 (grey lines), obtained using fluorogenic substrates for the different proteasomal activities. Results were plotted as percentage activity compared to non-treated lysates. Thick solid lines: tryptic activity; thin solid lines: chymotryptic activity; dotted lines: caspase-like activity. **B)** IC_{50} values of CEP-18770 (grey bars) and bortezomib (black bars) in RPMI8226, H929, JJN3 and HeLa cell lysates determined using fluorogenic substrates for the different proteasomal activities. IC_{50} values were determined in three independent experiments and error bars indicate SEM. • $p<0.05$

observed in JJN3 cells (Figure 2B).

Bortezomib and CEP-18770 show comparable inhibition patterns in cells

The proteasome inhibitory effects of bortezomib and CEP-18770 in intact RPMI8226, H929, and HeLa cells were investigated. To this end, active proteasome subunits in cells were labeled using a fluorescent proteasome activity probe (Me_4BodipyFL-Ahx$_3$Leu$_3$VS (**1**); Figure 1) that contains a vinyl sulfone reactive group that covalently modifies all N-terminal threonine residues of catalytically active proteasomal subunits, and a fluorescent tag that allows in-gel visualization of the subunit-probe complex in an SDS-PAGE gel. When one or more proteasome active sites are targeted by CEP-18770 or bortezomib treatment, probe labeling is hampered, resulting in a decrease in in-gel fluorescence intensity and ultimately in the disappearance of specific bands.[27]

Cells were pulsed for 1 h with increasing concentrations of bortezomib and CEP-18770, followed by a 2-h chase with probe **1**, a close analog of the bodipyFL probe described previously.[27] Cells were then lysed, subunits

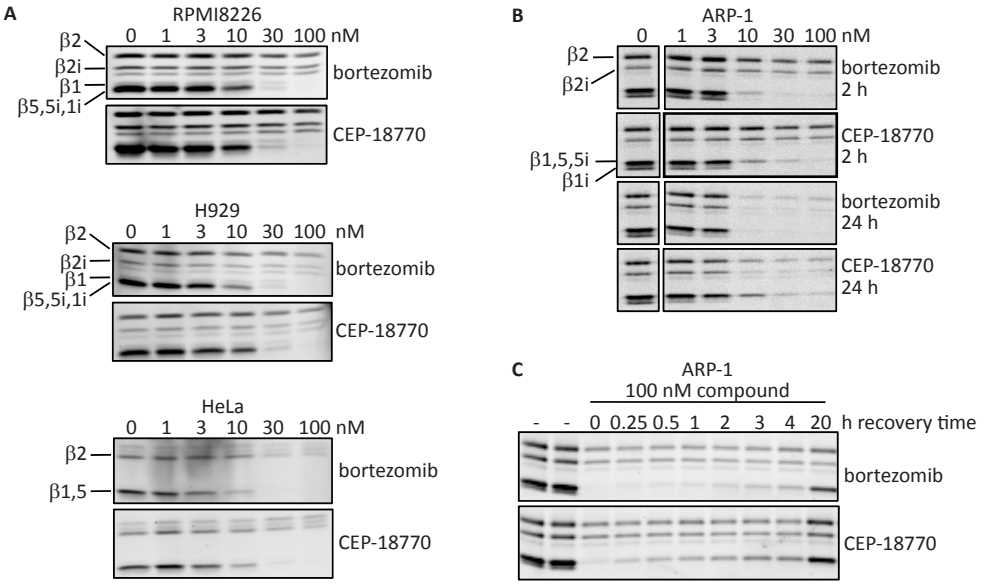

Figure 3 | Bortezomib and CEP-18770 induce near identical proteasome inhibition profiles and recovery patterns in live cells. A) In-gel fluorescence measurements showing representative proteasome activity profiles in RPMI8226, H929 and HeLa cells after a 1-hour incubation with increasing concentrations of bortezomib or CEP-18770. Results were obtained by incubating cells with inhibitor, followed by active proteasome labeling by probe **1**, and SDS-PAGE analysis. **B)** In-gel fluorescence measurements showing representative proteasome activity profiles in ARP-1 cells after a 2- or 24-hour incubation period with increasing concentrations of bortezomib and CEP-18770. Results were obtained by incubating cells with inhibitor, followed by active proteasome labeling by probe **1**, and SDS-PAGE analysis and fluorescence scanning. **C)** In-gel fluorescence measurements showing representative proteasome activity profiles in ARP-1 cells after a 1-hour incubation with 100 nM of bortezomib or CEP-18770, followed by the indicated recovery periods. Results were obtained by incubating cells with inhibitor, followed by active proteasome labeling by probe **1**, and SDS-PAGE analysis.

separated by SDS-PAGE and the gel scanned for fluorescence emission (Figure 3A). In untreated cells, the proteasome probe labeled all active subunits, and differences in subunit activity could be seen between different cell lines (Figure 3A, first lane). In H929 and RPMI8226 cells both constitutive and immunoproteasome subunits were active, as shown previously in RPMI8226 cells,[29] while in HeLa cells only constitutive subunits were labeled.[27,28] When cells were preincubated with either bortezomib or CEP-18770, the labeling of the β1 and β5 subunits disappeared in a concentration-dependent manner in all cell lines with estimated IC_{50} values in the low nanomolar range, while the labeling of the β2 subunits remained largely visible. These data confirm results in cell lysates and suggest that bortezomib and CEP-18770 are equipotent in inhibiting β1 and β5 subunits, but that they do not inhibit the β2 subunits in live cells.

Validating ARP-1 cells as a model system to compare bortezomib and CEP-18770 treatment *in vivo*

In a previous report, the *in vivo* efficacies of

CEP-18770 and bortezomib were compared in a RPMI8226 subcutaneous xenograft model of human MM, and in an ARP-1 systemic model of human MM.[25] In these models, differences were found between bortezomib and CEP-18770 in the extent and duration of tumor proteasome inhibition and antitumor efficacy. To assess whether the use of specific MM cell lines that respond differentially to CEP-18770 or bortezomib treatment were responsible for these observations, the effects of bortezomib and CEP-18770 were further studied in ARP-1 cells. ARP-1 cells were pulsed with increasing concentrations of bortezomib and CEP-18770 for 2 or 24 h, followed by a 2-h chase with proteasome probe **1**. Cells were then lysed, labeled subunits separated by SDS-PAGE and the resulting gel scanned for fluorescence emission. As can be seen in Figure 3B, both immuno- and constitutive proteasome subunits were labeled in untreated ARP-1 cells (Figure 3B, lane 1). In accord with results inform the RPMI8226, H929 and HeLa cells, bortezomib and CEP-18770 showed near identical inhibition profiles in ARP-1 cells (Figure 3B). After a 2-hour incubation period, both compounds dose-dependently inhibited β1 and β5 subunits with IC_{50} values between 3 and 10 nM, while β2 subunits remained relatively unaffected. Also after 24 h, both compounds inhibited β1 and β5 subunits, but in addition the labeling of β2 subunits was largely abolished at higher concentrations. As bortezomib and CEP-18870 do not interact with β2 subunits directly at the concentrations investigated (Figure 2A), this may be due to a secondary cellular response.

To investigate whether ARP-1 MM cells show differences in proteasome activity recovery after either bortezomib or CEP-18770 treatment, ARP-1 cells were pulsed for 1 h with 100 nM bortezomib or CEP-18770, washed and either probed directly (Figure 3C, lane 3), or allowed to recover for the indicated time periods before being analyzed. The patterns of activity recovery after withdrawal of either bortezomib or CEP-18770 were very similar (Figure 3C). After withdrawal of either inhibitor, proteasome activity recovered only slowly. After a 20-h recovery period, activity of the β5 subunits had not completely returned to baseline levels, while the activity of the β1i subunit was not detected (Figure 3C). These results indicate that although boronic-acid based proteasome inhibitors inhibit the proteasome in a reversible manner, proteasome synthesis, which occurs only after longer time periods, is the predominant factor contributing to recovery. Together, these data demonstrate that ARP-1 cells respond similarly to bortezomib and CEP-18770 treatment with respect to both proteasome inhibition and proteasome recovery patterns.

CEP-18770 shows an improved pharmacodynamic profile compared to bortezomib

To evaluate whether bortezomib and CEP-18770 show differences in proteasome inhibition *in vivo*, proteasome probe **1** was used to profile proteasome inhibition using an *ex vivo* approach.[27] NOD/SCID mice bearing subcutaneous ARP-1 tumor xenografts (n=5/group) were administered with the maximum tolerated dose (MTD) of bortezomib (1.2 mg/kg intravenous), CEP-18770 (4 mg/kg intravenous) or Solutol/PBS vehicle. At 2 h, 8 h or 24 h post dosing, mice were sacrificed and heart, lung, liver, spleen and tumor tissue obtained. Tissue cells were lysed, and lysates probed for proteasome activity, followed by SDS-PAGE. The resulting gels were scanned for fluorescence emission (Figure 4A) and the intensities of all bands were quantified using a sypro stain to control for protein loading. In all tissues, vehicle treatment had no effect on proteasomal subunit activity over a 24-h period (data not shown). Proteasome subunit activities in CEP-18770 and bortezomib treated samples were

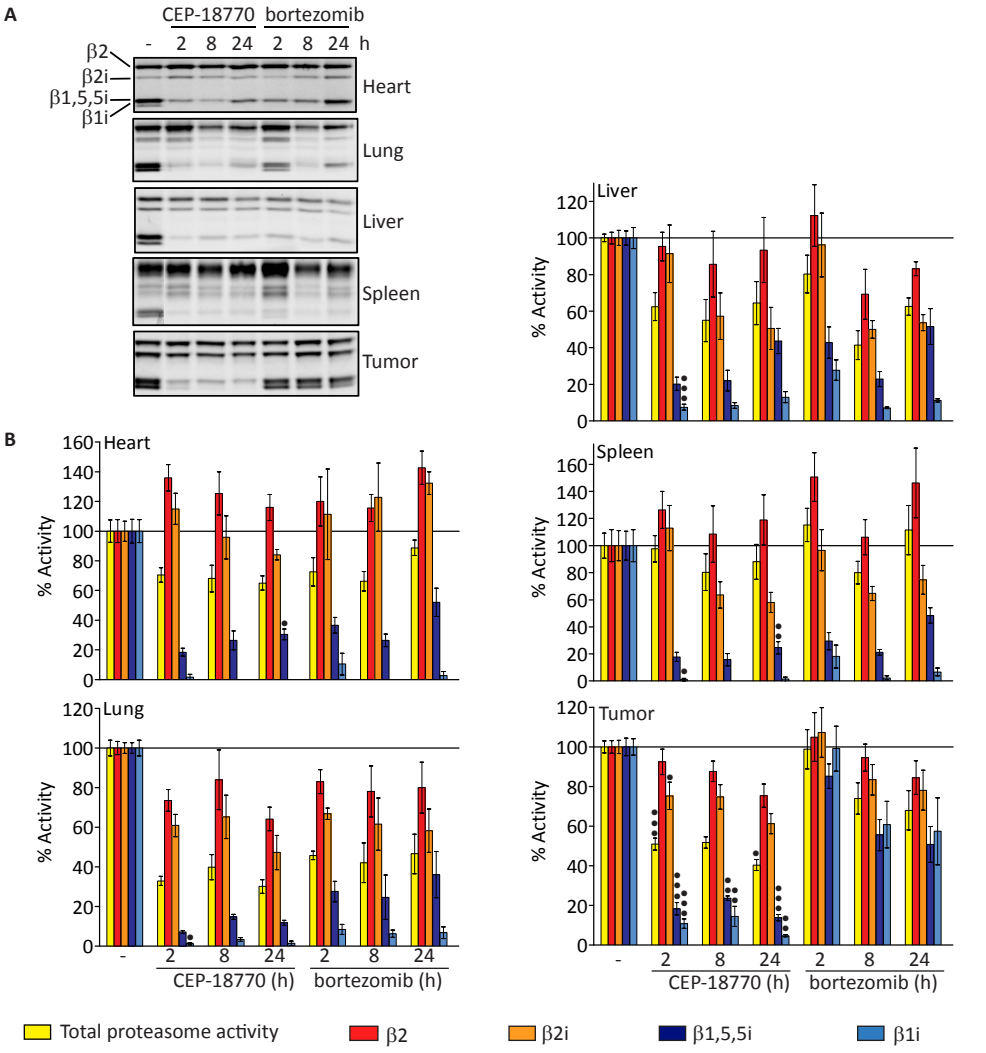

Figure 4 | CEP-18770 shows an improved pharmacodynamic profile compared to bortezomib in an ARP-1 MM tumor model. NOD/SCID mice (n=5/group) bearing ARP-1 tumor xenografts received a single injection of the maximum tolerated dose of bortezomib or CEP-18770 or vehicle, and tissues were removed at t = 2 h, 8 h, or 24 h post dosing. Tissues were lysed, followed by active proteasome labeling by probe **1** and SDS-PAGE analysis. **A)** In-gel fluorescence measurements showing representative proteasome activity profiles in mouse heart, lung, liver, spleen and tumor tissues after bortezomib or CEP-18770 treatment for the indicated time periods. **B)** Quantification of proteasome activity profiles in mouse heart, lung, liver, spleen and tumor tissues after bortezomib or CEP-18770 treatment for the indicated time periods. The proteasome subunit activity in treated samples was plotted as a percentage of the subunit activity in vehicle treated mice and total proteasome activity was defined as the sum of all individual activities. Error bars represent SEM. Statistical analysis was performed using GraphPad Prism software. CEP-18770 treated samples in which inhibition differed significantly from the corresponding bortezomib treated samples are indicated with dots. • $p<0.05$; •• $p<0.01$; ••• $p<0.001$

calculated as a percentage of the activities in vehicle-treated samples and averaged (Figure 4B). Total proteasome activity was defined as the sum of all individual activities.

In normal murine tissues, CEP-18770 and bortezomib showed comparable inhibition and recovery patterns, although subtle differences in inhibition patterns could be observed between the two inhibitors as well as between different tissue types. Bortezomib and CEP-18770 inhibited β1 and β5 subunits (Figure 4B, blue bars) to a similar degree in all tissues at all time points, with residual activities ranging between 20–50% for the β5,5i,1 subunits (dark blue bars) and 0–10% for the β1i subunit (light blue bars). The β2 subunit (red bars) was least affected by compound treatment. A small decrease in labeling was only observed in lung tissue. Labeling of the β2i subunit (orange bars) was decreased to a somewhat higher extent in lung, liver and spleen, predominantly at later time points. These results are in line with the results from ARP-1 cells (Figure 3B), suggesting that this was a secondary cellular response to proteasomal β1 and β5 subunit inhibition. Additional, little recovery of the activity of individual subunits was seen in this model over a period of 24 h, although in individual mice, proteasome activity appeared to recover in spleen, liver and heart after treatment with either compound (data not shown). Total proteasome activity (Figure 4B, yellow bars) was only partially inhibited in all normal tissues, predominantly because the β2,2i activities substantially contributed to total proteasome activity in all tissues examined (Figure 4A). The largest effects on total activity were observed in lung, where 40% residual proteasome activity was measured. In heart and liver, 60–70% of total proteasome activity remained after CEP-18770 and bortezomib treatment, while in spleen, total proteasome activity hardly decreased compared to vehicle (Figure 4B). No significant differences in total proteasome inhibition were observed between CEP-18770 and bortezomib in healthy murine tissue at all time points.

In ARP-1 tumor xenografts, differences between the inhibition produced by CEP-18770 and bortezomib were more pronounced. In primary tumor tissues β5 and β1 subunits were inhibited to a significantly higher extent by CEP-18770 treatment compared to bortezomib treatment at all time points, with residual activities ranging between 10–20% after CEP-18770 treatment and 60–80% after bortezomib treatment (Figure 4B). CEP-18770 induced maximal inhibition of these subunits within 2 h while maximal inhibition by bortezomib occurred only after 8–24 hours. Additionally, treatment with either compound resulted in small decreases in β2 and β2i labeling over time, as described above for normal tissues. As a result, the residual proteasome activity was significantly lower in CEP-18770-treated tumors as compared to bortezomib-treated tumors at 2 h and 24 h (Figure 4B). CEP-18770 reduced total proteasome activity to 40–50%, suggesting that this compound inhibited tumor proteasome to a similar or greater extent than proteasome in normal tissues. In contrast, the residual activity in bortezomib-treated tumor samples was 70–100%, suggesting that bortezomib inhibited proteasome activity in tumors to a lesser extent than in most normal tissues. Collectively, these data indicate that CEP-18770 induces a more favorable pharmacodynamic response in the ARP-1 MM tumor model as compared to bortezomib.

CEP-18770 displays activity against cells that are resistant to bortezomib

We next investigated whether CEP-18770 could overcome bortezomib resistance in the bortezomib resistant cell line THP1/BTZ_{100}.[30] THP1/BTZ_{100} cells acquired bortezomib resis-

tance by exposure to stepwise increasing concentrations of bortezomib (2.5 to 100 nM). Study of the molecular mechanism of bortezomib resistance in these cells revealed an Ala49Thr mutation in the β5 subunit protein.[30] This mutation has also been observed in Jurkat cells (human lymphoblastic T cells) with acquired bortezomib resistance.[31,32] THP1/BTZ_{100} cells were shown to be cross-resistant to other proteasome inhibitors that target the β5 subunit, including MG132, MG262 and 4A6.[30]

First, we compared the proteasome inhibitory potential of CEP-18770 and bortezomib in cell lysates of THP1/BTZ_{100} and THP1 wild type (THP1/WT) cells using fluorogenic substrates for the different proteasomal activities as described above. Lysates were pre-incubated for 1 hour with increasing concentrations of CEP-18770 and bortezomib after which residual proteasome activity was measured (Figure 5A) and IC_{50} values were calculated for the chymotryptic activity of the proteasome (Figure 5B). Bortezomib (black lines) and CEP-18770 (grey lines) showed near identical inhibition profiles in THP1/WT cells (dotted lines), in accordance with data obtained in other cell types (Figure 2A). Higher concentrations of bortezomib were required to inhibit the chymotryptic activity in THP1/BTZ_{100} cells as compared to THP1/WT cells, as expected (Figure 5A,B). Remarkably, CEP-18770 inhibited the chymoptryptic activity in THP1/BTZ_{100} cells with equal potency compared to the WT cell line (Figure 5A,B). In THP1/BTZ_{100} cells, no differences between bortezomib and CEP-18770 were observed in the degree of inhibition of the tryptic and caspase-like activities of the proteasome (Figure 5A).

Next, we set out to confirm that CEP-18770 was able to inhibit the β5 subunit in intact THP1/BTZ_{100} cells. To this end, THP1/WT and THP1/BTZ_{100} cells were pulsed with increasing concentrations of bortezomib and CEP-18770 for 3 or 24 h, followed by a 2-h chase with proteasome probe. Cells were then lysed, labeled subunits separated by SDS-PAGE and the resulting gel scanned for fluorescence emission. In line with results inform other cell lines tested, bortezomib and CEP-18770 showed near identical inhibition profiles in THP1/WT cells (Figure 5C, left panels). After a 3-hour incubation period, both compounds dose-dependently inhibited β1 and β5 subunits with IC_{50} values between 3 and 10 nM, while β2 subunits remained relatively unaffected. After 24 h, the labeling of β2 subunits by probe **1** was also hampered at higher concentrations of bortezomib and CEP-18770. In contrast, CEP-18770 and bortezomib showed different inhibition profiles in THP1/BTZ_{100} cells (Figure 5C, right panels). CEP-18770 inhibited the β5 subunits in THP1/BTZ_{100} cells with IC_{50} values between 3 and 10 nM, while higher concentrations of bortezomib were required to reach a similar extent of β5 inhibition. These differences are in accordance with results found in cell lysates using fluorogenic substrates and suggest that the β5 subunits in bortezomib resistant THP1 cells can still be inhibited by CEP-18770.

Finally, we investigated how the cell viability of THP1/BTZ_{100} and THP1/WT cells was influenced by bortezomib and CEP-18770 treatment. To this end, cells were exposed to increasing concentrations of bortezomib and CEP-18770 for 24 h or 48 h, after which cell viability was assessed using a cell titer blue assay. Values were normalized to control samples that were incubated with DMSO only and results were plotted as percentage compared to control values (Figure 5D). EC_{50} values, defined as the concentration of inhibitor causing 50% cell death, were determined at 48 h (Figure 5E). In accord with the proteasome inhibitory profiles found in these cells using probe **1**, THP1/WT cells responded similarly to bortezomib and CEP-18770 treatment

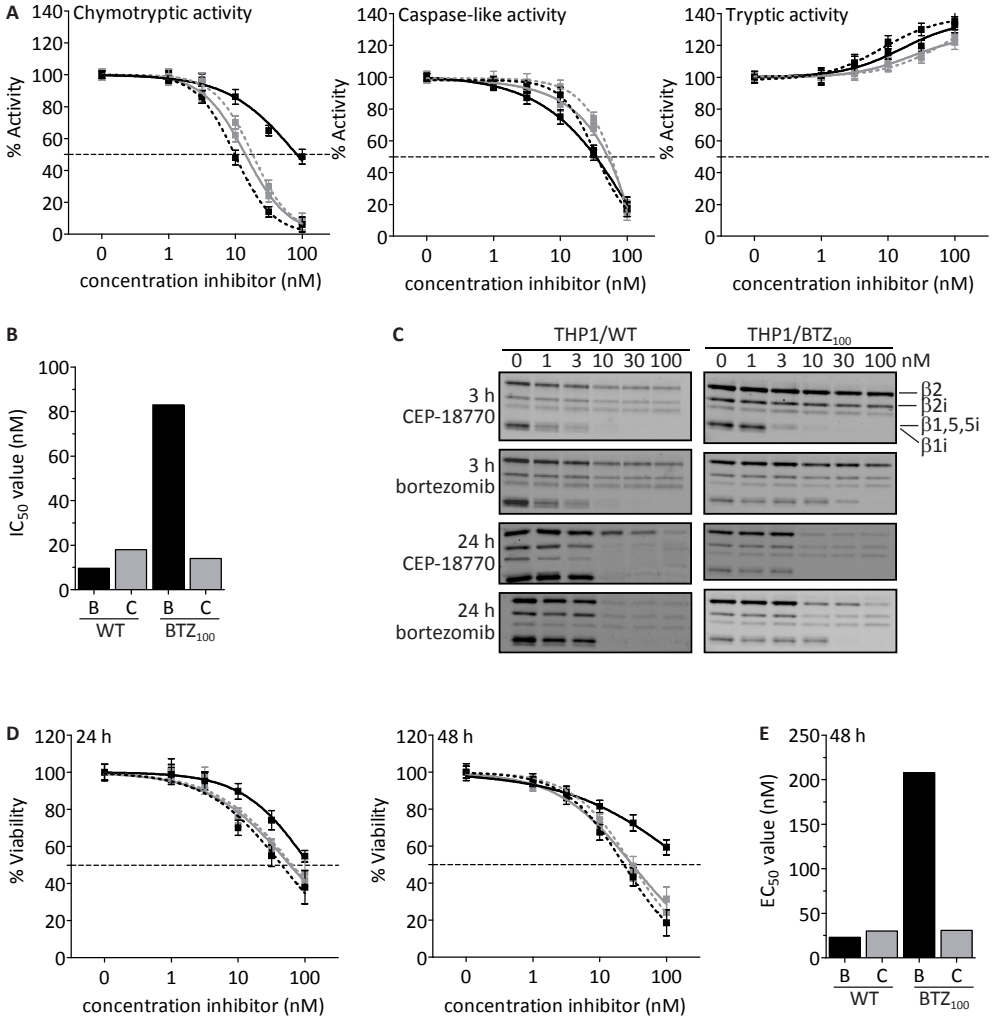

Figure 5 | CEP-18770 can overcome bortezomib resistance. A) Proteasome inhibitory profiles in THP1/WT and THP1/BTZ_{100} cell lysates after addition of increasing concentrations of bortezomib (black lines) or CEP-18770 (grey lines), obtained using fluorogenic substrates for the different proteasomal activities. Results were plotted as percentage activity compared to non-treated lysates. Solid lines: THP1/BTZ_{100} cells; dotted lines: THP1/WT cells. Error bars represent SEM of technical triplicates. **B)** IC_{50} values of CEP-18770 (grey bars) and bortezomib (black bars) in THP1/WT and THP1/BTZ_{100} cell lysates for inhibition of the chymotryptic activity. **C)** In-gel fluorescence measurements showing representative proteasome activity profiles in THP1/WT and THP1/BTZ_{100} cells after a 3 or 24-hour incubation with increasing concentrations of bortezomib or CEP-18770. Results were obtained by incubating cells with inhibitor, followed by active proteasome labeling by probe **1**, and SDS-PAGE analysis. **D)** Viability of THP1/WT and THP1/BTZ_{100} cells after incubation with increasing concentrations of bortezomib (black lines) or CEP-18770 (grey lines) for 24h or 48h. Results were plotted as percentage viability compared to a DMSO control. Solid lines: THP1/BTZ_{100} cells; dotted lines: THP1/WT cells. Error bars represent SEM of technical triplicates. **E)** EC_{50} values of CEP-18770 (grey bars) and bortezomib (black bars) in THP1/WT and THP1/BTZ_{100} cells.

(Figure 5D). In THP1/BTZ_{100} cells on the other hand, bortezomib showed higher EC_{50} values as compared to THP1/WT cells, whereas THP1/BTZ_{100} and THP1/WT cells were equally sensitive to CEP-18770 (Figure 5D,E). The EC_{50} value of CEP-18770 in THP1/BTZ_{100} cells was approximately 30 nM, whereas 100 nM bortezomib was not sufficient to kill 50% of all THP1/BTZ_{100} cells (Figure 5E). From the data obtained in THP1/BTZ_{100} and THP1/WT cells we conclude that THP1/BTZ_{100} cells are resistant to bortezomib due to a mutation in the β5 protein, which prevents bortezomib binding. Remarkably, THP1/BTZ_{100} cells are still equally sensitive to proteasome inhibition by CEP-18770 as compared to THP1/WT cells, and as a consequence, CEP-18770 displays similar EC_{50} values in THP1/BTZ_{100} and THP1/WT cells. Therefore, our data suggest that CEP-18770 can overcome acquired bortezomib resistance *in vitro*.

DISCUSSION

Proteasome inhibition is a validated strategy for the treatment of cancer, as evidenced by bortezomib, a boronic acid-based proteasome inhibitor, which is the active ingredient of velcade® and which is currently the only proteasome inhibitor approved for human use. Bortezomib treatment is however associated with adverse effects,[10] including thrombocytopenia[33] and peripheral neuropathy,[34] and with both primary and secondary resistance.[18] This has led to the search for new proteasome inhibitors with an improved cytotoxicity profile and the potential to overcome bortezomib resistance. CEP-18770, a novel proteasome inhibitor that is structurally similar to bortezomib, is one of several second-generation inhibitors in clinical trials.[24,25]

In the present study the proteasome inhibitory profiles of bortezomib and CEP-18770 were compared in cell lysates, whole cells and *ex vivo* in a mouse model of human MM, using both fluorogenic substrates and a chemical proteasome activity reporter that allows profiling of proteasome activity with high sensitivity in a wide range of cell types and tissues.[27] In addition, we investigated the proteasome inhibitory profiles of CEP-18770 and bortezomib in cells with acquired resistance to bortezomib, and assessed the effect of either CEP-18770 or bortezomib treatment on the cell viability of these cells.

CEP-18770 and bortezomib showed comparable inhibition patterns in a panel of human tumor cell lines. Both compounds were equipotent in inhibiting the β1 (caspase-like activity) and β5 (chymotryptic activity) subunits and had little effect on the β2 subunit activity (tryptic activity), in agreement with previous reports.[25,28] IC_{50} values in cell lysates were 40–75 nM and 10–25 nM for inhibition of the caspase-like and chymotryptic activity, respectively. In cell lines, IC_{50} values of both compounds for both the β1 and β5 subunits ranged between 3–10 nM. These data are in agreement with a previous report, in which bortezomib and CEP-18770 showed comparable effects in cells downstream of proteasome inhibition, including a comparable accumulation of polyubiquitinated proteins and the appearance of activated caspases-3, -7, and -9 with a comparable kinetic profile.[25] Data obtained using either fluorogenic substrates in cell lysates or using probe **1** in intact cells were similar, indicating the use of probe **1** provides a reliable method to assess proteasome activity.

Proteasome activity recovered similarly after withdrawal of either inhibitor from cells, with immediate but very slow recovery of β5(i)/1 subunit activity, and no recovery of the β1i activity within 20 hours. The slow rate of proteasome activity recovery after inhibition by either compound indicates that proteasome synthesis, and not the reversibility of boronic-

acid based proteasome inhibitors, is the predominant factor contributing to recovery, as suggested previously.[19] The factors contributing to a differential recovery of proteasomal activities are unknown, but differences in recovery between subunits have been reported.[22,35] After treatment with bortezomib, the recovery of caspase-like activity was delayed compared to that of chymotryptic activity.[22] Furthermore, continuous bortezomib treatment can abrogate immunoproteasome subunit expression and thus induce an altered subunit composition of newly synthesized proteasomes.[35]

In contrast to the finding that CEP-18770 and bortezomib have near identical effects on tumor cell proteasome activity *in vitro*, marked differences between CEP-18770 and bortezomib were found *in vivo* in an ARP-1 MM xenograft model. In tumor xenografts, CEP-18770 showed a significantly higher degree of inhibition of β1 and β5 subunits at all time points measured as compared to bortezomib (80–90% inhibition by CEP-18770 as compared to 40–60% inhibition by bortezomib), resulting in a significantly higher degree of overall proteasome inhibition (60% inhibition by CEP-18770 as compared to 32% inhibition by bortezomib), while the response of normal, healthy murine tissues to treatment with the maximum tolerated dose of bortezomib or CEP-18770 was near identical. CEP-18770 thus reduced proteasome activity in tumors to a greater extent than in most normal tissues, while bortezomib inhibited proteasome activity in tumors to a lesser extent than in most normal tissues, resulting in a favorable pharmacodynamic profile for CEP-18770 as compared to bortezomib. These results are in agreement with Piva et al., who have shown that in a RPMI8226 MM tumor xenograft model, CEP-18770 induced a similar degree of proteasome inhibition in normal mouse peripheral tissues compared to bortezomib, but a greater and more-sustained inhibition of tumor proteasome activity.[25] Consistent with these findings, CEP-18770 treatment has been shown to have a greater *in vivo* antitumor efficacy, and CEP-18770 administration resulted in a dose-related induction of complete tumor regression, whereas bortezomib treatment only delayed tumor growth.[25] Other studies have shown that bortezomib reduced proteasome activity in tumors to a lesser extent as compared to other tissues or whole blood samples[19,36,37] and similar observations have been reported for marizomib[38] and carfilzomib.[19] While the anti-tumor efficacy of bortezomib results in effective anti-tumor therapy, the improved response of CEP-18770 in tumors that can be correlated with its previously reported improved anti-tumor efficacy may result in further benefit in a clinical setting. In addition, the data obtained in mice *ex vivo* show that probe **1** can be successfully used for detailed studies of the effects of proteasome inhibitors on both normal and tumor tissues in preclinical models.

Finally, our data show that CEP-18770 displays activity against a bortezomib resistant cell line *in vitro*. The cell line THP1/BTZ_{100} is resistant to concentrations of bortezomib up to 100 nM. Study of the molecular mechanism of bortezomib resistance in these cells revealed an Ala49Thr mutation in the β5 subunit protein.[30] Ala49 is a highly conserved residue among many prokaryotic and mammalian species and very likely involved in tight interactions with the pyrazine-2-carboxyphenylalanyl backbone of bortezomib, as can be reasoned from the bortezomib liganded yeast 20S proteasome structure.[39] Therefore, mutation of this residue to threonine is likely to have a profound effect on binding of bortezomib and of other proteasome inhibitors that target the β5 subunit. Our data show that CEP-18770 binding was not influenced by the Ala49Thr mutation. Bortezomib and

CEP-18770 are structurally similar, but differ in their P2 and P3 residues, suggesting that even small changes to the backbone structure of bortezomib can be sufficient to overcome bortezomib resistance. The data presented here suggest that the development of second-generation proteasome inhibitors will likely result in the generation of inhibitors that can overcome resistance and may ultimately contribute to better patient outcome and that this outcome can be predicted with the use of activity reporter reagents.

MATERIALS AND METHODS

Reagents

The THP1/BTZ_{100} cell line was kindly provided by Dr. G. Jansen (VU University Medical Centre, Amsterdam, The Netherlands). Fluorogenic substrates were purchased from Bachem (Weil am Rhein, Germany). All solvents were purchased from Biosolve (Valkenswaard, the Netherlands) at the highest grade available. Bortezomib and CEP-18770 were synthesized at Cephalon Inc for this study. All other chemicals were purchased from Sigma-Aldrich (Zwijndrecht, the Netherlands) at the highest available purity.

Probe synthesis and characterization

Detailed information on synthetic procedures and characterization can be found in the Supplementary Information and Supplementary Schemes 1 and 2 therein.

Cell culture

RPMI8226 (human, multiple myeloma), ARP-1 (human, multiple myeloma), THP1/WT (human monocytic/macrophage) and H929 (human, multiple myeloma) cells were cultured in RPMI 1640 medium (Invitrogen). THP1/BTZ_{100} cells were cultured in RPMI 1640 medium supplemented with 100 nM bortezomib. JJN3 cells were cultured in RPMI 1640 medium containing 10mM HEPES (Invitrogen). HeLa cells (human, cervix carcinoma) were cultured in DMEM medium (Invitrogen). All media were supplemented with 10% fetal calf serum (FCS), 100 units/mL penicillin and 100 μg/mL streptomycin.

Inhibition experiments in cell lysates

Cells were washed with phosphate-buffered saline (PBS), pelleted and lysed with one volume of glass beads (<106 microns, acid-washed; Sigma) and an equal volume of homogenization buffer (50 mM Tris pH 7.4, 1 mM dithiothreitol (DTT), 5 mM $MgCl_2$, 2 mM ATP and 250 mM sucrose) by vortexing at high speed for 45 minutes at 4 °C. Beads, membrane fractions, nuclei and cell debris were then removed from the supernatant by centrifugation at 14,000 g for 5 minutes. Protein contents were quantified using the Bradford method (BioRad, Veenendaal, the Netherlands) or with a nanodrop spectrophotometer. Equal amounts of protein were incubated with 1, 3, 10, 30 or 100 nM bortezomib or CEP-18770 for 1 h at 37 °C. Control samples were incubated with 1 μM epoxomicin. To assay proteasome activity, 10 μg of lysate was added to 100 μL of substrate buffer (20 mM Tris pH 7.4, 5 mM $MgCl_2$, 1 mM DTT, 1 mM ATP and 100 μM BzValGlyArg-AMC (tryptic activity), 100 μM SucLeuLeuValTyr-AMC (chymotryptic activity) or 50 μM ZLeuLeuGlu-AMC (caspase-like activity)). Fluorescence was measured every minute for 25 minutes at 37 °C using a fluostar optima 96 well plate reader (BMG labtechnologies) (λ ex/em = 355/450 nm) and the increase in fluorescence per minute was used to calculate specific activities of each sample. Non-specific activities were determined using 1 μM epoxomicin, which specifically inhibits all proteasomal activity at this concentration, and the background signal obtained was subtracted from each measurement. IC_{50} values were determined in three independent experiments and averaged. Data were analyzed by using GraphPad Prism software (GraphPad, La Jolla, CA, USA).

Probing proteasome inhibition in whole cells

H929, RPMI8226, ARP-1 or HeLa cells (0.5×10^6 cells/mL) were pulsed with 0, 1, 3, 10, 30 or 100 nM bortezomib or CEP-18770 for 1, 2 or 24 hours at 37 °C, followed by a 2 hour chase with 500 nM proteasome activity probe **1**. Alternatively, ARP-1 cells were pulsed with 100 nM bortezomib or CEP-18770 for 1 hour, washed, and either chased directly with 500 nM proteasome activity probe 1 or left to recover for 0.25, 0.5, 1, 2, 3, 4 or 20 hours before being chased with probe **1**. THP1/WT or THP1/BTZ_{100} cells (0.5×10^6 cells/mL) were pulsed with 0, 1, 3, 10, 30 or 100 nM bortezomib

or CEP-18770 for 1 or 22 hours at 37 °C, followed by a 2 hour chase with 200 nM proteasome activity probe **1**. Cells were harvested, washed with cold PBS and lysed for 30 min. in NP40 lysis buffer (50 mM Tris pH 7.4, 150 mM NaCl, 1% NP40) at 4 °C. The Bradford assay was used to measure protein content.

***Ex vivo* evaluations**

Nod/Scid mice with established human ARP-1 MM subcutaneous tumor xenografts (n=5/group) were dosed at Cephalon (West Chester, PA) with the maximum tolerated dose of bortezomib (1.2 mg/kg i.v.), CEP-18770 (4 mg/kg i.v.) or Solutol/PBS vehicle. Experiments were approved by the Institutional Animal Care and Use Committee of Cephalon. At 2 h, 8 h, and 24 h post dosing heart, liver, lung, spleen and tumor tissue were obtained, rinsed in cold PBS and flash frozen in a tissue cassette under liquid N_2. Organs were lysed in homogenization buffer using glass beads as described above. Protein concentrations were determined using the Bradford assay, and equal amounts of protein were incubated with 1 μM probe **1** for 1 h at 37 °C. Statistical analyses were performed using by using GraphPad Prism software (GraphPad, La Jolla, CA, USA).

In-gel fluorescence measurements

Equal amounts of protein were denatured by boiling in LDS (Lithium dodecyl sulfate) sample buffer (Invitrogen) containing 2.5% β-mercaptoethanol and polypeptides were resolved by 12% SDS-PAGE using the NuPAGE system from invitrogen. Wet gel slabs were imaged for 2 min, with a resolution of 100 μm, using the ProXPRESS 2D Proteomic imaging system (Perkin Elmer), using appropriate filter settings (λ ex/em = 480/530 nm). To verify protein loading, gels were stained with ruthenium II tris bathophenanthroline disulfonate, as described,[40,41] and imaged using appropriate filter settings (λ ex/em = 460/680 nm). Probe signals were then normalized to the sypro signal. Images were analyzed using Totallab analysis software (Nonlinear Dynamics, Newcastle upon Tyne, UK) to quantify the intensity of the bands detected.

Cell viability assay

THP1/WT or THP1/BTZ_{100} cells (2×10^5 cells/mL were incubated with 0, 1, 3, 10, 30 or 100 nM bortezomib or CEP-18770 for 24 or 48 hours, followed by incubation with 20 μg/mL resazurin. The increase in fluorescence was measured after 8 hours using a PE envision plate reader. All results were expressed as percentage relative to untreated THP1/WT cells (100%).

ACKNOWLEDGMENTS

The authors thank Dr. G. Jansen for providing the THP1/BTZ_{100} cell line. This study was supported by the Dutch Cancer Society (grant number NKI 2005-3368) and by research funding from Cephalon to H.O.

REFERENCES

1. Adams, J. The development of proteasome inhibitors as anticancer drugs. *Cancer Cell.* **5**, 417-421 (2004).
2. Nalepa, G., Rolfe, M. & Harper, J.W. Drug discovery in the ubiquitin-proteasome system. *Nat. Rev. Drug Discov.* **5**, 596-613 (2006).
3. Dahlmann, B., Ruppert, T., Kuehn, L., Merforth, S. & Kloetzel, P.M. Different proteasome subtypes in a single tissue exhibit different enzymatic properties. *J. Mol. Biol.* **303**, 643-653 (2000).
4. Dahlmann, B., Ruppert, T., Kloetzel, P.M. & Kuehn, L. Subtypes of 20S proteasomes from skeletal muscle. *Biochimie.* **83**, 295-299 (2001).
5. Pelletier, S. et al. Quantifying cross-tissue diversity in proteasome complexes by mass spectrometry. *Mol. Biosyst.* (2010).
6. Raijmakers, R. et al. Automated online sequential isotope labeling for protein quantitation applied to proteasome tissue specific diversity. *Mol. Cell. Proteomics.* **7**, 1755-1762 (2008).
7. Adams, J. The proteasome: a suitable antineoplastic target. *Nat. Rev. Cancer.* **4**, 349-360 (2004).
8. Hideshima, T. et al. The proteasome inhibitor PS-341 inhibits growth, induces apoptosis, and overcomes drug resistance in human multiple myeloma cells. *Cancer Res.* **61**, 3071-3076 (2001).
9. Jagannath, S. et al. A phase 2 study of two doses of bortezomib in relapsed or refractory myeloma. *Br. J. Haematol.* **127**, 165-172 (2004).
10. Richardson, P.G. et al. A phase 2 study of bortezomib in relapsed, refractory myeloma. *N. Engl. J. Med.* **348**, 2609-2617 (2003).
11. Richardson, P.G. et al. Bortezomib or high-dose dexamethasone for relapsed multiple myeloma. *N. Engl. J. Med.* **352**, 2487-2498 (2005).
12. Fisher, R.I. et al. Multicenter phase II study of bortezomib in patients with relapsed or refractory

mantle cell lymphoma. *J. Clin. Oncol.* **24**, 4867-4874 (2006).
13. Orlowski, R.Z. et al. Phase 1 trial of the proteasome inhibitor bortezomib and pegylated liposomal doxorubicin in patients with advanced hematologic malignancies. *Blood.* **105**, 3058-3065 (2005).
14. Orlowski, R.Z. et al. Randomized phase III study of pegylated liposomal doxorubicin plus bortezomib compared with bortezomib alone in relapsed or refractory multiple myeloma: combination therapy improves time to progression. *J. Clin. Oncol.* **25**, 3892-3901 (2007).
15. Concannon, C.G. et al. Apoptosis induced by proteasome inhibition in cancer cells: predominant role of the p53/PUMA pathway. *Oncogene.* **26**, 1681-1692 (2007).
16. Richardson, P.G., Mitsiades, C., Hideshima, T. & Anderson, K.C. Bortezomib: proteasome inhibition as an effective anticancer therapy. *Annu. Rev. Med.* **57**, 33-47 (2006).
17. Nencioni, A., Grunebach, F., Patrone, F., Ballestrero, A. & Brossart, P. Proteasome inhibitors: antitumor effects and beyond. *Leukemia.* **21**, 30-36 (2007).
18. Orlowski, R.Z. & Kuhn, D.J. Proteasome inhibitors in cancer therapy: lessons from the first decade. *Clin. Cancer Res.* **14**, 1649-1657 (2008).
19. Demo, S.D. et al. Antitumor activity of PR-171, a novel irreversible inhibitor of the proteasome. *Cancer Res.* **67**, 6383-6391 (2007).
20. Kuhn, D.J. et al. Potent activity of carfilzomib, a novel, irreversible inhibitor of the ubiquitin-proteasome pathway, against preclinical models of multiple myeloma. *Blood.* **110**, 3281-3290 (2007).
21. Stapnes, C. et al. The proteasome inhibitors bortezomib and PR-171 have antiproliferative and proapoptotic effects on primary human acute myeloid leukaemia cells. *Br. J. Haematol.* **136**, 814-828 (2007).
22. Chauhan, D. et al. A novel orally active proteasome inhibitor induces apoptosis in multiple myeloma cells with mechanisms distinct from Bortezomib. *Cancer Cell.* **8**, 407-419 (2005).
23. Fenical, W. et al. Discovery and development of the anticancer agent salinosporamide A (NPI-0052). *Bioorg. Med. Chem.* **17**, 2175-2180 (2009).
24. Dorsey, B.D. et al. Discovery of a potent, selective, and orally active proteasome inhibitor for the treatment of cancer. *J. Med. Chem.* **51**, 1068-1072 (2008).
25. Piva, R. et al. CEP-18770: A novel, orally active proteasome inhibitor with a tumor-selective pharmacologic profile competitive with bortezomib. *Blood.* **111**, 2765-2775 (2008).
26. Sanchez, E. et al. The Novel Proteasome Inhibitor CEP-18770 Inhibits Myeloma Tumor Growth In Vitro and In Vivo and Enhances the Anti-MM Effects of Melphalan. *ASH Annual Meeting Abstracts.* **112**, 843 (2008).
27. Berkers, C.R. et al. Profiling proteasome activity in tissue with fluorescent probes. *Mol. Pharm.* **4**, 739-748 (2007).
28. Berkers, C.R. et al. Activity probe for in vivo profiling of the specificity of proteasome inhibitor bortezomib. *Nat. Methods.* **2**, 357-362 (2005).
29. Altun, M. et al. Effects of PS-341 on the activity and composition of proteasomes in multiple myeloma cells. *Cancer Res.* **65**, 7896-7901 (2005).
30. Oerlemans, R. et al. Molecular basis of bortezomib resistance: proteasome subunit beta5 (PSMB5) gene mutation and overexpression of PSMB5 protein. *Blood.* **112**, 2489-2499 (2008).
31. Lu, S. et al. Point mutation of the proteasome beta5 subunit gene is an important mechanism of bortezomib resistance in bortezomib-selected variants of Jurkat T cell lymphoblastic lymphoma/leukemia line. *J. Pharmacol. Exp. Ther.* **326**, 423-431 (2008).
32. Lu, S. et al. Different mutants of PSMB5 confer varying bortezomib resistance in T lymphoblastic lymphoma/leukemia cells derived from the Jurkat cell line. *Exp. Hematol.* **37**, 831-837 (2009).
33. Lonial, S. et al. Risk factors and kinetics of thrombocytopenia associated with bortezomib for relapsed, refractory multiple myeloma. *Blood.* **106**, 3777-3784 (2005).
34. Argyriou, A.A., Iconomou, G. & Kalofonos, H.P. Bortezomib-induced peripheral neuropathy in multiple myeloma: a comprehensive review of the literature. *Blood.* **112**, 1593-1599 (2008).
35. Fuchs, D., Berges, C., Opelz, G., Daniel, V. & Naujokat, C. Increased expression and altered subunit composition of proteasomes induced by continuous proteasome inhibition establish apoptosis resistance and hyperproliferation of Burkitt lymphoma cells. *J. Cell. Biochem.* **103**, 270-283 (2008).
36. Adams, J. et al. Proteasome inhibitors: a novel class of potent and effective antitumor agents. *Cancer Res.* **59**, 2615-2622 (1999).
37. LeBlanc, R. et al. Proteasome inhibitor PS-341 inhibits human myeloma cell growth in vivo and prolongs survival in a murine model. *Cancer Res.* **62**, 4996-5000 (2002).
38. Williamson, M.J. et al. Comparison of biochemical and biological effects of ML858 (salinosporamide A) and bortezomib. *Mol. Cancer Ther.* **5**, 3052-3061 (2006).
39. Groll, M., Berkers, C.R., Ploegh, H.L. & Ovaa, H. Crystal structure of the boronic acid-based proteasome inhibitor bortezomib in complex with the yeast 20S proteasome. *Structure.* **14**, 451-456 (2006).
40. Lamanda, A., Zahn, A., Roder, D. & Langen, H. Improved Ruthenium II tris (bathophenantroline disulfonate) staining and destaining protocol for a better signal-to-background ratio and improved baseline resolution. *Proteomics.* **4**, 599-608

(2004).
41. Rabilloud, T., Strub, J.M., Luche, S., van Dorsselaer, A. & Lunardi, J. A comparison between Sypro Ruby and ruthenium II tris (bathophenanthroline disulfonate) as fluorescent stains for protein detection in gels. *Proteomics.* **1**, 699-704 (2001).

Supplementary information

SUPPLEMENTARY METHODS

Fmoc peptide building blocks were from Novabiochem. All solvents were purchased from Biosolve at the highest grade available. All other chemicals were purchased from Aldrich at the highest available purity. All solvents and chemicals were used as received. L-Leucinyl vinyl sulfone was prepared as reported.[1-4] Nuclear magnetic resonance (NMR) spectra were recorded in the indicated solvent using a Bruker Avance 300 (^{1}H: 300 MHz; ^{13}C: 75 MHz) spectrometer. LC-MS analyses were carried out on a WATERS LCT mass spectrometer in line with a WATERS 2795 HPLC system and a WATERS 2996 photodiode array detector. Reversed phase runs were performed on a 3 μm Atlantis T3, C18 RP, 2.1 x 100 mm column (Waters) using gradient elution with H_2O/0.1% formic acid as solvent A and acetonitrile/0.1% formic acid as solvent B at a flow rate of 0.4 mL/min. Reversed phase HPLC runs were performed on a Waters 1525 EF HPLC system in line with a Waters 2487 dual λ absorbance detector using gradient elution with H_2O/0.05% TFA as solvent A and acetonitrile/0.05% TFA as solvent B. Analytical runs were performed on a 10 μm 4.6x150 mm Atlantis dC18 column (Waters) at a flow rate of 1.4 ml/min and preparative runs were performed on a 10 μm 19x250 mm Atlantis dC18 column (Waters) at a flow rate of 18 mL/min.

Synthesis of Me_4BodipyFL-NHS ester (Supplementary Scheme 1)

I: (Z)-tert-butyl 2-(hydroxyimino)-3-oxobutanoate (1)

A solution of sodium nitrite (1.4 g, 20.3 mmol) in deionized water was added dropwise over 5 minutes to a stirred mixture of *tert*-butyl acetoacetate (2.80 g, 17.4 mmol) in acetic acid (4 mL), while keeping the reaction vessel in an ice-bath. The reaction mixture was stirred at 4 °C for an additional 16 hours.

II: tert-butyl 4-(3-methoxy-3-oxopropyl)-3,5-dimethyl-1H-pyrrole-2-carboxylate (2)

The resulting solution containing oxime **1** was slowly added in 5 portions to a solution of methyl 4-acetyl-5-oxohexanoate (5 mL, 28.6 mmol) in acetic acid (15 mL) kept at 65 °C. Simultaneously, a mixture of zinc dust (3 g, 45.9 mmol) and sodium acetate (3 g, 36.6 mmol) was added in portions such that zinc/sodium acetate was in excess of dione. After stirring the mixture for 2 more hours at 65 °C it was poured into ice water and left slowly stirring for 16 hours, allowing the mixture to warm up to room temperature. The precipitate, including product and zinc residues was filtered off using a glass filter. The residue was taken up in ethyl acetate (100 mL) and the organic layer was dried with magnesium sulfate ($MgSO_4$). The $MgSO_4$ was filtered off and the filtrate was concentrated *in vacuo* to dryness, yielding tetrasubstituted pyrrole **2** as a light brown solid (2.87 g, 10.2 mmol, 59 % yield), which was used without further purification in the next step.

III: Methyl 3-(5-formyl-2,4-dimethyl-1H-pyrrol-3-yl)propanoate (3)

Pyrrole **2** (1 g, 3.55 mmol) was dissolved in TFA (20 mL) and stirred for 20 minutes on ice. Triethylorthoformate (2 mL, 12 mmol) was added slowly and the solution was stirred gently at 0 °C for 15 minutes. Water (2 mL) was added and the solution was stirred for 10 minutes at 0 °C. The solution was coevaporated with toluene *in vacuo* to dryness at room temperature. The crude product was purified by flash column chromatography using ethyl acetate as the eluent to yield aldehyde **3** as a brown solid (469 mg, 2.25 mmol, 63 % yield).

IV: (Z)-2-((3,5-dimethyl-2H-pyrrol-2-ylidene) methyl)-4-(3-methoxy-3-oxopropyl)-3,5-dimethyl-1H-pyrrol-1-ium (4)

Aldehyde **3** (469 mg, 2.25 mmol) was dissolved in absolute ethanol (8 mL) and cooled to 0 °C. 2,4-dimethylpyrrole (256 mg, 2.69 mmol) was added under an argon atmosphere and 4 mL of cold 4N HCl in dioxane was added. After Stirring for 15 minutes at 0 °C, the solution was transferred to a 50 mL Falcon tube and centrifuged at 1500g for 10 minutes at 4 °C. The supernatant was discarded and the resulting orange solid was

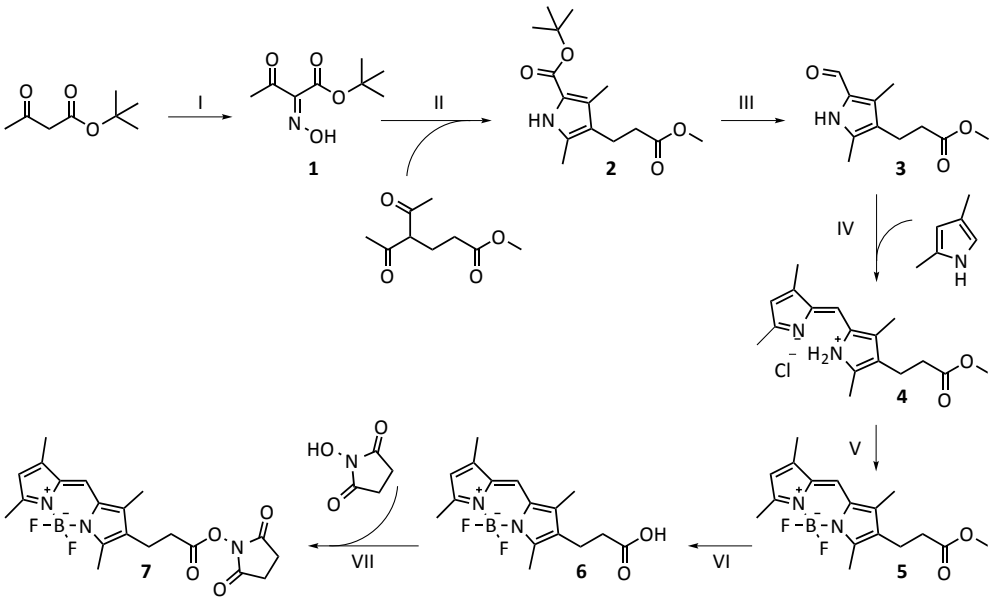

Supplementary Scheme 1 | Synthesis of Me_4BodipyFL-NHS ester 7. Step numbers correspond to step numbers outlined in the text.

resuspended in cold diethylether (40 mL) and centrifuged again. The supernatant was decanted and the residue was dried under a stream of nitrogen, yielding crude dipyrrole **4** as an orange solid, which was used in the next step without further purification.

V: Me_4BodipyFL-methyl ester (5)

Dipyrrole **4** was suspended in 1,2-dichlorobenzene (20 mL) under an argon atmosphere and triethylamine (1 mL, 7.16 mmol) and boron trifluoride diethyl etherate (1 mL, 8.12 mmol) were added in concert. The resulting metallic solution was stirred for 30 minutes at 100 °C and allowed to cool to room temperature. The solution was diluted with dry hexanes (25 mL) and applied directly onto a silica gel column for purification by flash column chromatography using 25% EtOAc in toluene as the eluent to afford Me_4BodipyFL-methyl ester **5** as an orange solid (481 mg, 1.44 mmol, 64 % yield starting from aldehyde **3**).

VI: Me_4BodipyFL-OH (6)

Me_4BodipyFL-methyl ester **5** (400 mg, 1.24 mmol) was dissolved in ethanol (6 mL) and 1 M lithium hydroxide (LiOH) solution was added (1.3 mL). The solution was stirred until TLC (eluent: EtOAc containing 0.1% acetic acid) revealed complete conversion. Ethyl acetate (40 mL) and 0.1 M HCl (30 mL) were added and the two layers were separated. The organic layer was dried with $MgSO_4$ and concentrated *in vacuo* to dryness to obtain an orange solid. Purification by flash column chromatograpy using EtOAc containing 0.1% acetic acid as the eluent afforded Me_4BodipyFL-OH **6** as an orange solid (306 mg, 0.95 mmol, 77 % yield). ^{1}H NMR ($CDCl_3$): δ 7.09 (s, 1H), 6.10 (s, 1H), 2.66 (dd, *J*=8.2 Hz, *J*=7.1 Hz, 2H), 2.59 (s, 6H), 2.60-2.53 (m, 2H), 2.31 (s, 3H), 2.27 (s, 3H). ^{13}C NMR ($CDCl_3$): δ 178.2 (CO), 156.5 (C_q), 155.3 (C_q), 141.0 (C_q), 138.1 (C_q), 133.3 (C_q), 132.6 (C_q), 127.8 (C_q), 119.7 (CH), 118.9 (CH), 33.9 (CH_2), 19.2 (CH_2), 14.6 (CH_3), 12.7 (CH_3), 11.2 (CH_3), 9.6 (CH_3).

VII: Me_4BodipyFL-NHS ester (7)

Me_4BodipyFL-OH **6** (306 mg, 0.95 mmol) was dissolved in dichloromethane (60 mL) and N-hydroxy succinimide (120 mg, 1.05 mmol), EDCI (201 mg, 1.05 mmol) and DMAP (11 mg, 0.1 mmol) were added. The mixture was stirred for

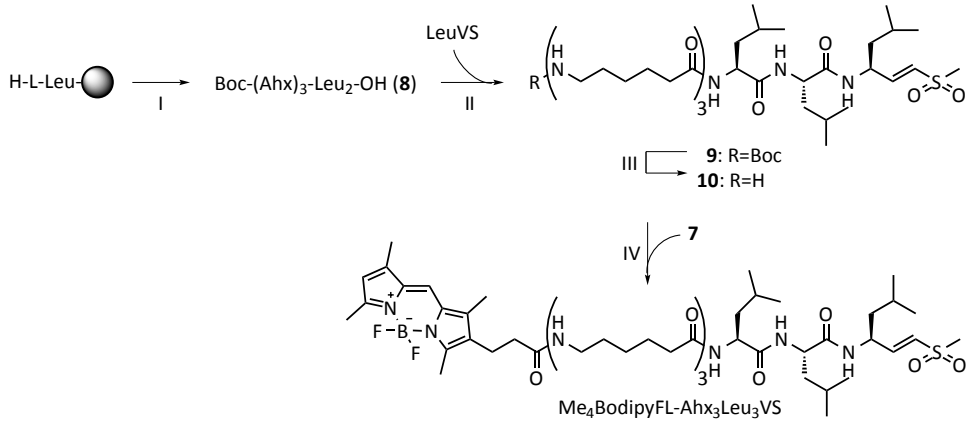

Supplementary Scheme 2 | Synthesis of Me_4BodipyFL-Ahx_3Leu_3VS. Step numbers correspond to step numbers outlined in the text.

16 hours at room temperature, 0.05 M HCl (40 mL) was added the two layers separated. The organic layer was dried with $MgSO_4$ and concentrated *in vacuo* to dryness to obtain an orange solid, which was purified by flash column chromatography using EtOAc : hexanes (2:3 v/v) as the eluent to obtain Me_4BodipyFL-NHS ester **7** as a dark orange solid (242 mg, 0.85 mmol) in 61 % yield. ^{1}H NMR ($CDCl_3$): δ 7.02 (s, 1H), 6.02 (s, 1H), 2.85-2.78 (m, 6H), 2.75-2.70 (m, 2H), 2.50 (s, 6H), 2.22 (s, 3H), 2.19 (s, 3H). ^{13}C NMR ($CDCl_3$): δ 169.0 (2xCO), 167.7 (CO), 156.9 (C_q), 154.8 (C_q), 141.3 (C_q), 138.0 (C_q), 133.4 (C_q), 132.5 (C_q), 126.7 (C_q), 119.9 (CH), 119.0 (CH), 31.1 (CH_2), 25.6 (2xCH_2), 19.2 (CH_2), 14.6 (CH_3), 12.6 (CH_3), 11.2 (CH_3), 9.6 (CH_3).

Synthesis of Me_4BodipyFL-Ahx_3Leu_3VS (Supplementary Scheme 2)

The synthesis of H_2N-Ahx_3Leu_2-OH involving standard Fmoc-based solid-phase peptide synthesis (SPPS) protocols and the subsequent coupling of fluorescent dye and vinyl sulfone electrophile to yield the final proteasome probe are depicted in Scheme 2.

I: Boc-Ahx_3Leu_2OH (8)

Hyper acid-labile H-Leu-2-ClTrt resin (novabiochem) (1 g, 0.3 mmol equivalents) was subjected to four coupling cycles, in which deprotection of the Fmoc-group with piperidine/NMP (1:4 v/v; 10 mL/g of dry resin), was followed by a coupling cycle with 3 equivalents of Fmoc-protected amino acid, 3 equivalents of DIPEA and 3 equivalents of PyBop coupling reagent in NMP (10 mL/g of dry resin). Coupling steps were performed with Fmoc-Leu-OH (1x), Fmoc-6-aminohexanoic acid (Fmoc-Ahx-OH) (2x) and Boc-Ahx-OH (1x) sequentially. The peptide was cleaved from the resin using 2% TFA in dichloromethane and the compound was concentrated under reduced pressure. The product was purified by flash column chromatography using a gradient of 10 % to 20% MeOH in CH_2Cl_2 containing 0.1 % acetic acid as the eluent to obtain Boc-Ahx_3Leu_2OH **8** as a white solid (205 mg, 0.3 mmol) in > 80 % yield.

II: Boc-Ahx_3Leu_3VS (9)

L-Leucinyl vinyl sulfone (LeuVS, 50 mg, 0.26 mmol) was dissolved in DMF and Boc-Ahx_3Leu_2OH **8** (116 mg, 0.17 mmol), DIPEA (89 μL, 0.51 mmol) and EDCI (50 mg, 0.26 mmol) were added. The solution was stirred for 3 hours at room temperature and then concentrated *in vacuo* to dryness to yield an off-white solid. The product was purified by flash column chromatography using 10 % MeOH in CH_2Cl_2 as the eluent to obtain Boc-Ahx_3-Leu_3VS **9** as a white solid (103 mg, 0.12 mmol) in 71 % yield.

III: H_2N-Ahx_3Leu_3VS (10)

Boc-Ahx_3Leu_3VS **9** (12 mg, 14 μmol) was dissolved in TFA (1 mL) and left at room temperature for 30 minutes. The product was precipitated by adding cold diethylether (40 mL) and isolated by centrifugation at 1000g (low brake speed) for 5 minutes at 4 ˚C to afford H_2N-Ahx_3Leu_3VS **10** as a white solid (10.6 mg, 14 μmol) in > 98 % yield.

IV: Me_4BodipyFL-Ahx_3Leu_3VS

H_2N-Ahx_3Leu_3VS **10** (10.6 mg, 14 μmol) was dissolved in DMF (1 mL) and Me_4BodipyFL-NHS ester **7** (6.4 mg, 15.5 μmol) and DIPEA (24 μL, 0.14 mmol) were added. The resulting solution was stirred at room temperature for 16 hours. The solution was concentrated *in vacuo* to dryness and purify by reversed phase HPLC to obtain the fluorescent proteasome probe Me_4BodipyFL-Ahx_3Leu_3VS (6 mg, 5.7 μmol) in 40% yield. MS (ESI): 1058.66 $(M+H)^+$; 520.27 $(M+H-F)^{2+}$; 1080.91 $(M+Na)^+$

SUPPLEMENTARY REFERENCES

1. Bogyo, M. et al. Covalent modification of the active site threonine of proteasomal beta subunits and the Escherichia coli homolog HslV by a new class of inhibitors. *Proc Natl Acad Sci U S A* **94**, 6629-6634 (1997).
2. Palmer, J.T., Rasnick, D., Klaus, J.L. & Bromme, D. Vinyl sulfones as mechanism-based cysteine protease inhibitors. *J. Med. Chem.* **38**, 3193-3196 (1995).
3. Rydzewski, R. et al. Optimization of Subsite Binding to the â5 Subunit of the Human 20S Proteasome Using Vinyl Sulfones and 2-Keto-1,3,4-oxadiazoles: Syntheses and Cellular Properties of Potent, Selective Proteasome Inhibitors. *J. Med. Chem.* **49**, 2953-2968 (2006).
4. Wang, G., Mahesh, U., Chen, G.Y. & Yao, S.Q. Solid-phase synthesis of peptide vinyl sulfones as potential inhibitors and activity-based probes of cysteine proteases. *Org. Lett.* **5**, 737-740 (2003).